IEICE TRANSACTIONS

on Communications

VOL. E101-B NO. 7
JULY 2018

A PUBLICATION OF THE COMMUNICATIONS SOCIETY

The Institute of Electronics, Information and Communication Engineers
Kikai-Shinko-Kaikan Bldg., 5-8, Shibakoen 3chome, Minato-ku, TOKYO, 105-0011 JAPAN

IEICE TRANS. COMMUN., VOL.E101–B, NO.7 JULY 2018

PAPER

Analysis of a Wireless Power Transfer System by the Impedance Expansion Method Using Fourier Basis Functions

Nozomi HAGA[†a)], ***Member and*** **Masaharu TAKAHASHI**[††b)], ***Fellow***

SUMMARY The impedance expansion method (IEM), which has been previously proposed by the authors, is a circuit-modeling technique for electrically-very-small devices. This paper provides a new idea on the principle of undesired radiation in wireless power transfer systems by employing IEM. In particular, it is shown that the undesired radiation is due to equivalent infinitesimal dipoles and loops of the currents on the coils.

key words: *wireless power transfer, method of moments, impedance expansion method, Fourier basis functions*

1. Introduction

Wireless power transfer (WPT) technology [1] will be applied to various devices such as low-power mobile terminals and high-power electric vehicles, and many WPT studies are being conducted in various research fields including power electronics, antenna engineering, and electromagnetic compatibility. Regardless of the field, it is important to understand the operating principle of the coupling devices (coils or antennas) to make them efficient and reduce undesired radiation.

In this regard, the impedance expansion method (IEM), which is a circuit-modeling technique for electrically-very-small devices, was proposed by the authors [2], [3]. In the IEM, self- and mutual impedances in the method of moments (MoM) [4] are expanded into the Laurent series with respect to the complex angular frequency $s = j\omega$, and the terms that are proportional to s^{-1} and s are represented by capacitors and inductors, respectively, whereas the higher-degree terms are represented by dependent voltage sources.

This paper provides a new idea on the principle of undesired radiation in WPT systems by employing IEM. In a similar research, Hirayama et al. have reported that the radiation in WPT systems can be explained by equivalent electric dipoles of the currents on the coils [5]. On the other hand, this paper shows that the radiation in WPT systems can be explained by introducing equivalent infinitesimal loops in addition to the equivalent infinitesimal dipoles.

Because IEM is based on the MoM, the current distributions on conductors are expanded into a set of basis functions. In this paper, the Fourier basis functions are employed because of the following characteristics:

1. The required number of unknowns (basis functions) is expected to be small because the current distributions on the coils are approximately sinusoidal.
2. Some of the self- and mutual impedance components between basis functions can be calculated analytically, and this is useful for understanding the operation principle of the system.

Among them, the second point is important to discuss the behaviors of the equivalent infinitesimal dipoles and loops.

This paper is organized as follows. Section 2 describes the analysis model and the Fourier basis functions dealt with in this paper. Section 3 describes the self- and mutual impedances between the basis functions. Section 4 describes the system of linear equations to be solved and the procedure to obtain S-parameters, radiated power, and conduction loss power. Section 5 describes a numerical example. Section 6 concludes the paper.

2. Analysis Model

2.1 Structure of the Model

Figure 1 shows the WPT system discussed in this paper. Each transmitting (Tx) and receiving (Rx) side consists of a feeding loop and a resonance coil, and they are symmetrically placed with respect to the xy-plane of $z = 0$. The parameters

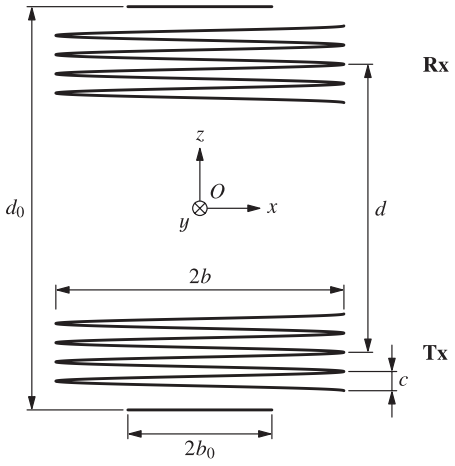

Fig. 1 WPT system.

Manuscript received August 15, 2017.
Manuscript revised November 28, 2017.
Manuscript publicized January 18, 2018.

[†]The author is with the Graduate School of Science and Technology, Gunma University, Kiryu-shi, 376-8585 Japan.
[††]The author is with the Center for Frontier Medical Engineering, Chiba University, Chiba-shi, 263-8522 Japan.
a) E-mail: nozomi.haga@gunma-u.ac.jp
b) E-mail: omei@m.ieice.org

DOI: 10.1587/transcom.2017EBP3316

representing the dimensions of the system are defined as follows:

- a radius of the wires,
- b_0 radius of the loops,
- b radius of the coils,
- c pitch of the coils,
- d_0 distance between the Tx and Rx loops,
- d distance between the Tx and Rx coils,
- N number of turns of the coils.

The positions on the central axes of the respective elements can be expressed in terms of a parametric variable u as follows:

1. Position on the Tx loop:

$$\boldsymbol{r}(u) = \hat{x} b_0 \cos(2\pi u) + \hat{y} b_0 \sin(2\pi u) - \hat{z} d_0/2, \quad (1)$$

where $0 \le u \le 1$.
2. Position on the Tx coil:

$$\boldsymbol{r}(u) = \hat{x} b \cos(2\pi u) + \hat{y} b \sin(2\pi u) + \hat{z}[c(u - N/2) - d/2], \quad (2)$$

where $0 \le u \le N$.
3. Position on the Rx loop:

$$\boldsymbol{r}(u) = \hat{x} b_0 \cos(2\pi u) + \hat{y} b_0 \sin(2\pi u) + \hat{z} d_0/2, \quad (3)$$

where $0 \le u \le 1$.
4. Position on the Rx coil:

$$\boldsymbol{r}(u) = \hat{x} b \cos(2\pi u) + \hat{y} b \sin(2\pi u) - \hat{z}[c(u - N/2) - d/2], \quad (4)$$

where $0 \le u \le N$.

2.2 Basis Functions

In the IEM analysis used in this paper, the current distributions on the loops and the coils are approximated to be filamentary along the wire axis, i.e. this is the so-called thin-wire approximation.

Because the dimensions of the loops are much smaller than the wavelength, the current distributions on the loops are assumed to be uniform along the axis of the wire. In other words, the basis function for the Tx loop $\boldsymbol{F}_{T0}(u)$ and that for the Rx loop $\boldsymbol{F}_{R0}(u)$ are as follows:

$$\boldsymbol{F}_{T0}(u) = \boldsymbol{F}_{R0}(u) = -\hat{x} \sin(2\pi u) + \hat{y} \cos(2\pi u). \quad (5)$$

On the other hand, the current distributions on the coils are expanded into a set of Fourier basis functions, as described earlier. The definition of the basis function for the Tx coil $\boldsymbol{F}_{Tm}(u)$ and that for the Rx coil $\boldsymbol{F}_{Rm}(u)$ are as follows:

$$\boldsymbol{F}_{Tm}(u) = \frac{-\hat{x} \sin(2\pi u) + \hat{y} \cos(2\pi u) + \hat{z} h}{\sqrt{1 + h^2}} \sin\Big(\frac{m\pi u}{N}\Big), \quad (6)$$

$$\boldsymbol{F}_{Rm}(u) = \frac{-\hat{x} \sin(2\pi u) + \hat{y} \cos(2\pi u) - \hat{z} h}{\sqrt{1 + h^2}} \sin\Big(\frac{m\pi u}{N}\Big), \quad (7)$$

where $m \ge 1$ and $h = c/(2\pi b)$. Using the Fourier basis functions, the current on the Tx coil $\boldsymbol{I}_T(u)$ and that on the Rx coil $\boldsymbol{I}_R(u)$ are expanded as follows:

$$\boldsymbol{I}_T(u) = \sum_{m=1}^{N_F} I_{Tm} \boldsymbol{F}_{Tm}(u), \quad (8)$$

$$\boldsymbol{I}_R(u) = \sum_{m=1}^{N_F} I_{Rm} \boldsymbol{F}_{Rm}(u), \quad (9)$$

where N_F is the maximum degree of the Fourier series, and I_{Tm} and I_{Rm} are the current coefficients for $\boldsymbol{F}_{Tm}(u)$ and $\boldsymbol{F}_{Rm}(u)$, respectively.

3. Self- and Mutual Impedances between Basis Functions

In this paper, the self- and mutual impedances are denoted in a way such that: $Z_{T0,T0}$ is the self-impedance of the basis function $\boldsymbol{F}_{T0}$, $Z_{Tm,Rn}$ is the mutual impedance between the basis functions $\boldsymbol{F}_{Tm}$ and $\boldsymbol{F}_{Rn}$, and so on. In the IEM, the self- and mutual impedances are expanded into the Laurent series such that:

$$Z_{Tm,Tn} \simeq \sum_{i=-1}^{N_L} s^i Z_{Tm,Tn}^{(i)}, \quad (10)$$

$$Z_{Tm,Rn} \simeq \sum_{i=-1}^{N_L} s^i Z_{Tm,Rn}^{(i)}, \quad (11)$$

where N_L is the maximum degree of the Laurent series, $Z_{Tm,Tn}^{(i)}$ and $Z_{Tm,Rn}^{(i)}$ are constants independent of s, and $m \ge 0$ and $n \ge 0$. In [2], it has been shown that the self-impedance component that is proportional to s^2 corresponds to the radiation resistance of an infinitesimal dipole of which length is equal to the integrated value of the basis function. In addition, this section shows that the self-impedance component that is proportional to s^4 corresponds to the radiation resistance of an equivalent infinitesimal loop of the basis function.

3.1 Integral Representations

According to the reciprocity theorem and the geometrical symmetry between the Tx and Rx sides, the expressions for the self- and mutual impedances between the basis functions can be consolidated into the following six integral representations. Here, ζ is the wave impedance, v is the propagation velocity of the electromagnetic waves, and R is the distance between the source and the observation points, which shall be offset by the radius a if they are on the same element.

1. Self-impedance of the basis function on the loop:

$$Z^{(i)}_{T0,T0} = Z^{(i)}_{R0,R0} = \frac{(-1)^{i-1}\zeta}{(i-1)!4\pi v^i}\int_0^1\int_0^1 (2\pi b_0)^2\cos[2\pi(u-u')]R^{i-2}du'du, \quad (12)$$

where $i \geq 1$ and

$$R = \sqrt{a^2 + 4b_0^2\sin^2[\pi(u-u')]}. \quad (13)$$

2. Mutual impedance between the basis functions on the loop and the coil at the same side:

$$Z^{(i)}_{T0,Tm} = Z^{(i)}_{Tm,T0} = Z^{(i)}_{R0,Rm} = Z^{(i)}_{Rm,R0} = \frac{(-1)^{i-1}\zeta}{(i-1)!4\pi v^i}\int_0^1\int_0^N (2\pi)^2 b_0 b\cos[2\pi(u-u')]\sin\Big(\frac{m\pi u'}{N}\Big)R^{i-2}du'du, \quad (14)$$

where $m \geq 1$, $i \geq 1$, and

$$R = \sqrt{(b_0-b)^2 + 4b_0 b\sin^2[\pi(u-u')] + [c(2u'-N) + d_0 - d]^2/4}. \quad (15)$$

3. Self-/mutual impedance between the basis functions on the same coil:

$$Z^{(-1)}_{Tm,Tn} = Z^{(-1)}_{Tn,Tm} = Z^{(-1)}_{Rm,Rn} = Z^{(-1)}_{Rn,Rm} = \frac{\zeta v}{4\pi}\int_0^N\int_0^N \frac{mn\pi^2}{N^2}\cos\Big(\frac{m\pi u}{N}\Big)\cos\Big(\frac{n\pi u'}{N}\Big)\frac{1}{R}du'du, \quad (16)$$

$$Z^{(i)}_{Tm,Tn} = Z^{(i)}_{Tn,Tm} = Z^{(i)}_{Rm,Rn} = Z^{(i)}_{Rn,Rm} = \frac{(-1)^{i-1}\zeta}{(i-1)!4\pi v^i}\int_0^N\int_0^N \{(2\pi b)^2\cos[2\pi(u-u')] + c^2\}\sin\Big(\frac{m\pi u}{N}\Big)\sin\Big(\frac{n\pi u'}{N}\Big)R^{i-2}du'du + \frac{(-1)^{i+1}\zeta}{(i+1)!4\pi v^i}\int_0^N\int_0^N \frac{mn\pi^2}{N^2}\cos\Big(\frac{m\pi u}{N}\Big)\cos\Big(\frac{n\pi u'}{N}\Big)R^i du'du, \quad (17)$$

where $m \geq 1$, $n \geq 1$, $i \geq 1$, and

$$R = \sqrt{a^2 + 4b^2\sin^2[\pi(u-u')] + c^2(u-u')^2}. \quad (18)$$

4. Mutual impedance between the basis functions on the different loops:

$$Z^{(i)}_{T0,R0} = Z^{(i)}_{R0,T0} = \frac{(-1)^{i-1}\zeta}{(i-1)!4\pi v^i}\int_0^1\int_0^1 (2\pi b_0)^2\cos[2\pi(u-u')]R^{i-2}du'du, \quad (19)$$

where $i \geq 1$ and

$$R = \sqrt{4b_0^2\sin^2[\pi(u-u')] + d_0^2}. \quad (20)$$

5. Mutual impedance between the basis functions on the loop and the coil at the opposite sides:

$$Z^{(i)}_{T0,Rm} = Z^{(i)}_{Rm,T0} = Z^{(i)}_{R0,Tm} = Z^{(i)}_{Tm,R0} = \frac{(-1)^{i-1}\zeta}{(i-1)!4\pi v^i}\int_0^1\int_0^N (2\pi)^2 b_0 b\cos[2\pi(u-u')]\sin\Big(\frac{m\pi u'}{N}\Big)R^{i-2}du'du, \quad (21)$$

where $m \geq 1$, $i \geq 1$, and

$$R = \sqrt{(b_0-b)^2 + 4b_0 b\sin^2[\pi(u-u')] + [c(2u'-N) - d_0 - d]^2/4}. \quad (22)$$

6. Mutual impedance between the basis functions on the different coils:

$$Z^{(-1)}_{Tm,Rn} = Z^{(-1)}_{Rn,Tm} = Z^{(-1)}_{Rm,Tn} = Z^{(-1)}_{Tn,Rm} = \frac{\zeta v}{4\pi}\int_0^N\int_0^N \frac{mn\pi^2}{N^2}\cos\Big(\frac{m\pi u}{N}\Big)\cos\Big(\frac{n\pi u'}{N}\Big)\frac{1}{R}du'du, \quad (23)$$

$$Z^{(i)}_{Tm,Rn} = Z^{(i)}_{Rn,Tm} = Z^{(i)}_{Rm,Tn} = Z^{(i)}_{Tn,Rm} = \frac{(-1)^{i-1}\zeta}{(i-1)!4\pi v}\int_0^N\int_0^N \{(2\pi b)^2\cos[2\pi(u-u')] - c^2\}\sin\Big(\frac{m\pi u}{N}\Big)\sin\Big(\frac{n\pi u'}{N}\Big)R^{i-2}du'du + \frac{(-1)^{i+1}\zeta}{(i+1)!4\pi v^i}\int_0^N\int_0^N \frac{mn\pi^2}{N^2}\cos\Big(\frac{m\pi u}{N}\Big)\cos\Big(\frac{n\pi u'}{N}\Big)R^i du'du, \quad (24)$$

where $m \geq 1$, $n \geq 1$, $i \geq 1$, and

$$R = \sqrt{4b^2\sin^2[\pi(u-u')] + [c(u+u'-N) - d]^2}. \quad (25)$$

3.2 Closed-Form Expressions for Even-Degree Components

Among the impedance components described here, those in which i is even can be integrated analytically. Here, let us consider several important components.

(1) Components of $i = 2$

The self- and mutual impedance components between the basis functions on the loops are zero, as follows:

$$Z^{(2)}_{T0,T0} = Z^{(2)}_{T0,R0} = 0. \quad (26)$$

This means that no electric dipole is constructed by $\boldsymbol{F}_{T0}$ and $\boldsymbol{F}_{R0}$.

On the other hand, the self- and mutual impedances between the basis functions on the same coil are nonzero if both m and n are odd or $m = n = 2N$. For example, the self-impedance component of $m = n = 1$ is as follows:

$$Z^{(2)}_{T1,T1} = -\frac{\zeta}{6\pi v^2}\Big[b^2\frac{16N^2}{(4N^2-1)^2} + c^2\frac{4N^2}{\pi^2}\Big]. \quad (27)$$

It is notable that $s^2 Z^{(2)}_{T1,T1}$ is equivalent to the radiation resistance of an infinitesimal dipole [6] with the length

$$l = \sqrt{b^2 \frac{16N^2}{(4N^2-1)^2} + c^2 \frac{4N^2}{\pi^2}}. \tag{28}$$

Similarly, the mutual impedance components between the basis functions on the different coils are nonzero if both m and n are odd or $m = n = 2N$. For example, the mutual impedance component of $m = n = 1$ is as follows:

$$Z^{(2)}_{T1,R1} = -\frac{\zeta}{6\pi v^2}\left[b^2 \frac{16N^2}{(4N^2-1)^2} - c^2 \frac{4N^2}{\pi^2}\right]. \tag{29}$$

If the absolute value of the second term in the brackets is larger than that of the first term, $s^2 Z^{(2)}_{T1,R1} < 0$. This means that the equivalent infinitesimal dipoles of $\boldsymbol{F}_{T1}$ and $\boldsymbol{F}_{R1}$ are oriented so that their radiations are canceled partially.

(2) Components of $i = 4$

The self- and mutual impedance components between the basis functions on the loops are as follows:

$$Z^{(4)}_{T0,T0} = Z^{(4)}_{T0,R0} = \frac{\zeta}{6v^4}\pi b_0^4. \tag{30}$$

It is notable that $s^4 Z^{(4)}_{T0,T0}$ is equivalent to the radiation resistance of an infinitesimal loop [6] with the radius b_0. In addition, because $s^4 Z^{(4)}_{T0,R0} > 0$, the equivalent infinitesimal loops of $\boldsymbol{F}_{T0}$ and $\boldsymbol{F}_{R0}$ are oriented so that their radiations are enhanced.

On the other hand, the self- and mutual impedance components between the basis functions on the same coil are nonzero except if only one of either m or n is even. For example, the self-impedance component of $m = n = 1$ is as follows:

$$\begin{aligned} Z^{(4)}_{T1,T1} = \frac{\zeta}{30\pi v^4}\Bigg\{ & -a^2 b^2 \frac{16N^2}{(4N^2-1)^2} - a^2 c^2 \frac{4N^2}{\pi^2} \\ & + b^4\left[20N^2 - \frac{32N^2}{(4N^2-1)^2} + \frac{12N^2}{(16N^2-1)^2}\right] \\ & + b^2 c^2\left[-\frac{8N^2}{\pi^2} + \frac{8N^2(208N^4-8N^2+1)}{(4N^2-1)^4\pi^2}\right. \\ & \left. - \frac{8N^4}{(4N^2-1)^2}\right] - c^4\left(\frac{1}{\pi^2} - \frac{8}{\pi^4}\right)N^4\Bigg\} \\ \simeq & \frac{2\zeta}{3\pi v^4} b^4 N^2, \end{aligned} \tag{31}$$

where the last approximation holds true when $b \gg a$, $b \gg c$, and $N \gg 1$. It should be noted that the approximate expression for $s^4 Z^{(4)}_{T1,T1}$ is equivalent to the radiation resistance of an infinitesimal loop with the radius b and turns $(2/\pi)N$. Here, $2/\pi$ is the mean value of $\sin(\pi u/N)$, which is contained in $\boldsymbol{F}_{T1}$, in the range $0 \le u \le N$. Therefore, the behavior of $s^4 Z^{(4)}_{T1,T1}$ can be considered to be similar to that of the radiation resistance of an infinitesimal loop.

Moreover, the mutual impedance components between the basis functions on the different coils are basically nonzero. For example, the mutual impedance component of $m = n = 1$ is as follows:

$$\begin{aligned} Z^{(4)}_{T1,R1} = \frac{\zeta}{30\pi v^4}\Bigg\{ & b^4\left[20N^2 - \frac{32N^2}{(4N^2-1)^2} + \frac{12N^2}{(16N^2-1)^2}\right] \\ & + b^2 c^2\left[\frac{8N^2}{\pi^2} + \frac{8N^2(16N^4+16N^2-1)}{(4N^2-1)^4\pi^2}\right. \\ & \left. - \frac{8N^4}{(4N^2-1)^2}\right] - b^2 d^2 \frac{16N^2}{(4N^2-1)^2} \\ & + c^4\left(\frac{1}{\pi^2} - \frac{8}{\pi^4}\right)N^4 + c^2 d^2 \frac{2N^2}{\pi^2}\Bigg\} \\ \simeq & \frac{2\zeta}{3\pi v^4} b^4 N^2, \end{aligned} \tag{32}$$

where the last approximation holds true when $b \gg a$, $b \gg c$, and $N \gg 1$, and is the same as that for the self-impedance component $Z^{(4)}_{T1,T1}$. In addition, because $s^4 Z^{(4)}_{T1,R1} > 0$, the equivalent infinitesimal loops of $\boldsymbol{F}_{T1}$ and $\boldsymbol{F}_{R1}$ are oriented so that their radiations are enhanced.

3.3 Components Due to Surface Impedance of Conductors

Because conduction loss is not negligible in usual WPT systems, the impedance components due to the surface impedance of conductors $\zeta_c = \sqrt{s\mu/\sigma}$ should be added to the self- and mutual impedances described in the previous section. Here, μ and σ are the permeability and conductivity of conductors, respectively.

Such components between the basis functions that do not overlap each other are zero. Also, according to the orthogonality of sinusoidal functions, the components of $m \neq n$ are zero. Therefore, only the self-impedance components should be taken into account. In particular, the respective components are as follows.

1. Self-impedance of the basis function on the loops:

$$Z^c_{T0,T0} = Z^c_{R0,R0} = \zeta_c \frac{b_0}{a}. \tag{33}$$

2. Self-impedance of the basis function on the coils:

$$Z^c_{Tm,Tm} = Z^c_{Rm,Rm} = \zeta_c \frac{N\sqrt{(2\pi b)^2 + c^2}}{4\pi a}, \tag{34}$$

where $m \ge 1$.

4. System of Linear Equations to be Solved

This paper discusses the S-parameters, the radiated power, and the conduction loss power when two ports are mounted on the Tx and Rx loops. In this case, the system of linear equations to be solved is as follows:

$$\sum_{n=0}^{N_F}\sum_{i=-1}^{N_L} s^i Z^{(i)}_{Tm,Tn} I_{Tn} + \sum_{n=0}^{N_F}\sum_{i=-1}^{N_L} s^i Z^{(i)}_{Tm,Rn} I_{Rn}$$

$$+ Z^c_{Tm,Tm} I_{Tm} = V_{Tm}, \quad m = 0, \ldots, N_F, \tag{35}$$

$$\sum_{n=0}^{N_F} \sum_{i=-1}^{N_L} s^i Z^{(i)}_{Rm,Tn} I_{Tn} + \sum_{n=0}^{N_F} \sum_{i=-1}^{N_L} s^i Z^{(i)}_{Rm,Rn} I_{Rn} + Z^c_{Rm,Rm} I_{Rm} = V_{Rm}, \quad m = 0, \ldots, N_F, \tag{36}$$

$$V_{T0} = V_0 - R_0 I_{T0}, \tag{37}$$

$$V_{R0} = -R_0 I_{R0}, \tag{38}$$

$$V_{Tm} = V_{Rm} = 0, \quad m = 1, \ldots, N_F, \tag{39}$$

where R_0 is the characteristic impedance of the ports, and V_0 is the electromotive force of the Tx port and can be expressed in terms of the available power P_a as $V_0 = 2\sqrt{R_0 P_a}$.

In terms of the current coefficients, which are the solutions of Eqs. (35)–(39), the S-parameters can be calculated as follows:

$$S_{11} = 1 - \frac{2R_0 I_{T0}}{V_0}, \quad S_{21} = -\frac{2R_0 I_{R0}}{V_0}. \tag{40}$$

In addition, the radiated power P_r can be obtained as the sum of subcomponents due to the respective self-/mutual impedance components:

$$P^{(i)}_{r,Tm,Tm} = s^i Z^{(i)}_{Tm,Tm} |I_{Tm}|^2, \tag{41}$$

$$P^{(i)}_{r,Tm,Tn} = s^i Z^{(i)}_{Tm,Tn} \mathrm{Re}(2 I_{Tm} I^*_{Tn}), \quad m < n, \tag{42}$$

$$P^{(i)}_{r,Rm,Rm} = s^i Z^{(i)}_{Rm,Rm} |I_{Rm}|^2, \tag{43}$$

$$P^{(i)}_{r,Rm,Rn} = s^i Z^{(i)}_{Rm,Rn} \mathrm{Re}(2 I_{Rm} I^*_{Rn}), \quad m < n, \tag{44}$$

$$P^{(i)}_{r,Tm,Rn} = s^i Z^{(i)}_{Tm,Rn} \mathrm{Re}(2 I_{Tm} I^*_{Rn}), \tag{45}$$

$$P^{(i)}_r = \sum_{m=0}^{N_F} \sum_{n=m}^{N_F} P^{(i)}_{r,Tm,Tn} + \sum_{m=0}^{N_F} \sum_{n=m}^{N_F} P^{(i)}_{r,Rm,Rn} + \sum_{m=0}^{N_F} \sum_{n=0}^{N_F} P^{(i)}_{r,Tm,Rn}, \tag{46}$$

$$P_r = P^{(2)}_r + P^{(4)}_r + \cdots, \tag{47}$$

where the asterisks denote the complex conjugates. For example, $P^{(i)}_{r,Tm,Tm}$ is the subcomponent due to the self-impedance component $Z^{(i)}_{Tm,Tm}$. As for the case $i = 2$, the relation $P^{(2)}_{r,Tm,Tm} \geq 0$ holds true because $s^2 Z^{(2)}_{Tm,Tm} \geq 0$. Similarly, in the case $i = 4$, the relation $P^{(4)}_{r,Tm,Tm} \geq 0$ holds true if $s^4 Z^{(4)}_{Tm,Tm} \geq 0$. In contrast, the subcomponent $P^{(i)}_{r,Tm,Rn}$, for example, may be negative, depending on the sign of $s^i Z^{(i)}_{Tm,Rn}$ and the phase relation of the current coefficients I_{Tm} and I_{Rn}. In this case, the radiations due to I_{Tm} and I_{Rn} are canceled partially. In addition, $P^{(i)}_r$ is the sum of the subcomponents due to impedance components that are proportional to s^i.

On the other hand, the conduction loss power P_c can be calculated as follows:

$$P_{c,Tm,Tm} = \mathrm{Re}(Z^c_{Tm}) \, |I_{Tm}|^2, \tag{48}$$

$$P_{c,Rm,Rm} = \mathrm{Re}(Z^c_{Rm}) \, |I_{Rm}|^2, \tag{49}$$

$$P_c = \sum_{m=0}^{N_F} P_{c,Tm,Tm} + \sum_{m=0}^{N_F} P_{c,Rm,Rm}. \tag{50}$$

5. Numerical Example

5.1 Calculation Conditions

Discussions in the remaining sections are made based on the numerical results with the following condition:

$a = 0.8\,\mathrm{mm}$, $b_0 = 93\,\mathrm{mm}$, $b = 118\,\mathrm{mm}$,
$c = 8\,\mathrm{mm}$, $d_0 = 280\,\mathrm{mm}$, $d = 200\,\mathrm{mm}$,
$N = 10$, $\sigma = 58\,\mathrm{MS/m}$.

These parameters were determined so that the transmission coefficient $|S_{21}|$ in the 50-Ω system is maximum at around 13.56 MHz. In addition, the available power of the Tx port is assumed to be $P_a = 1\,\mathrm{W}$.

As for the analysis condition, the maximum degrees of the Fourier and Laurent series were set to $N_F = 25$ and $N_L = 4$, respectively. In this case, the total radiated power can be obtained as $P_r = P^{(2)}_r + P^{(4)}_r$. It has already been confirmed that the calculated results have almost converged under this condition. For example, the maximum difference between $|S_{11}|$ when $N_F = 25$ and 27 is 0.383 dB in the frequency range 12–15 MHz. Moreover, the maximum difference between P_r when $N_L = 4$ and 6 is 8.31×10^{-4} dB in the same frequency range.

Incidentally, the double integrals in the expressions for the self- and mutual impedance components were numerically calculated using the tanh-sinh quadrature [7]. Among the numerical results, the components of even i were compared with those obtained by the analytical expressions. As a result, it has been confirmed that the numerical results have approximately 10-digit accuracy.

In addition, the same problem was analyzed by means of a usual full-wave MoM to validate the results by the IEM. In the full-wave MoM used here, the current distributions on the wires are represented by surface currents, instead of the thin-wire approximation. The surface of the wires is divided into quadrangular segments. The division number along the circumference direction is 12 whereas that along the axial direction is 48 per 1 turn. The details about the basis functions are described in the Appendix. In addition, the feeding ports are positioned at $u = 0$ on the loops.

5.2 Calculated Results

Figure 2 plots the frequency dependences of (a) $|S_{11}|$, (b) $|S_{21}|$, (c) P_r, and (d) P_c, where the markers denoted by "MoM" indicate the results by the full-wave MoM for comparison. Regarding (c) P_r, the components $P^{(2)}_r$ and $P^{(4)}_r$ obtained by the IEM are plotted in addition to the total power. All the results obtained by the IEM and the full-wave MoM agree with each other. The slight discrepancy in P_c is because the variation of the current density along the circumference direction of the wire is ignored in the IEM because of the thin-wire approximation. However, the results

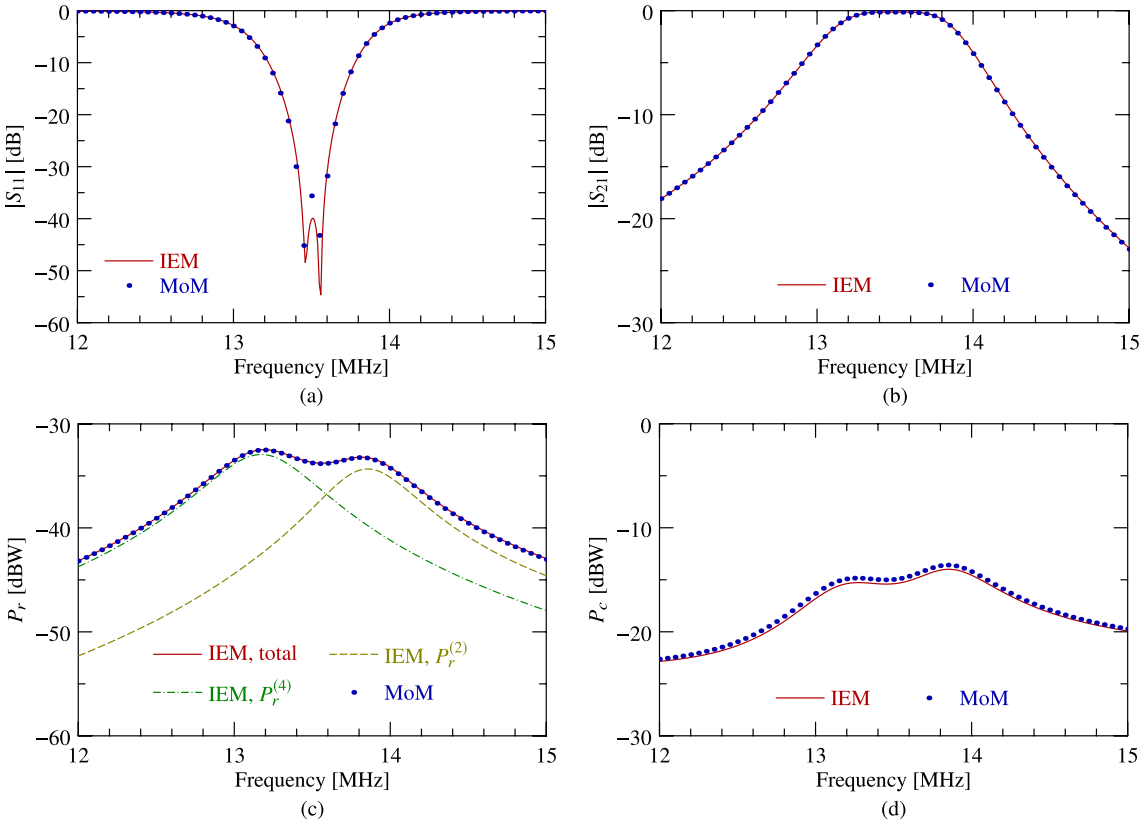

Fig. 2 Frequency dependences of (a) $|S_{11}|$, (b) $|S_{21}|$, (c) P_r, and (d) P_c.

by the IEM can be considered to be reasonable because the difference is less than 0.51 dB.

Now, we focus on the fact that $P_r^{(2)}$ and $P_r^{(4)}$ are maximum at different frequencies, namely 13.85 MHz and 13.17 MHz, respectively. To clarify the reason, the subcomponents of $P_r^{(2)}$ and $P_r^{(4)}$ are discussed here. Table 1 shows several low-degree components of $P_r^{(2)}$, where the components known to be zero are not shown. In both the frequencies, the absolute values of the following components are superior to those of the other components:

- $P^{(2)}_{r,T1,T1}$, which is determined by the magnitude of I_{T1},
- $P^{(2)}_{r,R1,R1}$, which is determined by the magnitude of I_{R1},
- $P^{(2)}_{r,T1,R1}$, which is determined by the magnitudes and the phase relation of I_{T1} and I_{R1}.

Here, it should be noted that $P^{(2)}_{r,T1,R1}$ is negative at 13.17 MHz and is positive at 13.85 MHz. Because the calculated value of the related mutual impedance component is $Z^{(2)}_{T1,R1} \simeq 5.45685\times10^{-19}\,\Omega\cdot\mathrm{s}^2$, $s^2 Z^{(2)}_{T1,R1} < 0$. As described earlier, this means that the equivalent infinitesimal dipoles of the basis functions $\boldsymbol{F}_{T1}$ and $\boldsymbol{F}_{R1}$ are oriented so that their radiations are canceled partially. Besides, the phase difference between I_{T1} and I_{R1} is approximately 46° at 13.17 MHz and is approximately 137° at 13.85 MHz. Therefore, the radiation is partially canceled at 13.17 MHz and is enhanced at 13.85 MHz. This is consistent with the results shown in Table 1.

Subsequently, Table 2 shows several low-degree components of $P_r^{(4)}$, where the components known to be zero or less than 10^{-10} W are not shown. In both the frequencies, the absolute values of the following components are superior to those of the other components:

- $P^{(4)}_{r,T1,T1}$, which is determined by the magnitude of I_{T1},
- $P^{(4)}_{r,R1,R1}$, which is determined by the magnitude of I_{R1},
- $P^{(4)}_{r,T1,R1}$, which is determined by the magnitudes and the phase relation of I_{T1} and I_{R1}.

Here, it should be noted that $P^{(4)}_{r,T1,R1}$ is positive at 13.17 MHz and is negative at 13.85 MHz. This relation is opposite to that of $P^{(2)}_{r,T1,R1}$. Because the calculated value of the related mutual impedance component is $Z^{(4)}_{T1,R1} \simeq 1.91939\times10^{-34}\,\Omega\cdot\mathrm{s}^4$, $s^2 Z^{(4)}_{T1,R1} > 0$. As described earlier, this means that the equivalent infinitesimal loops of the basis functions $\boldsymbol{F}_{T1}$ and $\boldsymbol{F}_{R1}$ are oriented so that their radiations are enhanced. According to the phase difference between I_{T1} and I_{R1} described earlier, the radiation is enhanced at 13.17 MHz and is partially canceled at 13.85 MHz. This is consistent with the results shown in Table 2.

In addition, because the total radiated power $P_r = P_r^{(2)} + P_r^{(4)}$ obtained by the IEM agrees with that by the full-wave MoM, it can be concluded that the undesired radiations in the WPT system consist of the radiations due to the equivalent dipoles and loops of the currents on the coils.

Table 1 Subcomponents of $P_r^{(2)}$ (Unit: [W]).

	13.17 MHz	13.85 MHz
$P^{(2)}_{r,T1,T1}$	1.01137×10^{-4}	1.45124×10^{-4}
$P^{(2)}_{r,T1,T3}$	9.04016×10^{-6}	1.24252×10^{-5}
$P^{(2)}_{r,T1,T5}$	2.73084×10^{-6}	3.76786×10^{-6}
$P^{(2)}_{r,T3,T3}$	5.28422×10^{-7}	6.95677×10^{-7}
$P^{(2)}_{r,T3,T5}$	5.00880×10^{-7}	6.61958×10^{-7}
$P^{(2)}_{r,T5,T5}$	1.28353×10^{-7}	1.70284×10^{-7}
$P^{(2)}_{r,R1,R1}$	5.09615×10^{-5}	6.88061×10^{-5}
$P^{(2)}_{r,R1,R3}$	4.55032×10^{-6}	5.89852×10^{-6}
$P^{(2)}_{r,R1,R5}$	1.37378×10^{-6}	1.78993×10^{-6}
$P^{(2)}_{r,R3,R3}$	2.65693×10^{-7}	3.30673×10^{-7}
$P^{(2)}_{r,R3,R5}$	2.51703×10^{-7}	3.14864×10^{-7}
$P^{(2)}_{r,R5,R5}$	6.44640×10^{-8}	8.10529×10^{-8}
$P^{(2)}_{r,T1,R1}$	-8.91319×10^{-5}	1.31858×10^{-4}
$P^{(2)}_{r,T1,R3}$	-1.49265×10^{-6}	2.12755×10^{-6}
$P^{(2)}_{r,T1,R5}$	2.38393×10^{-7}	-3.42316×10^{-7}
$P^{(2)}_{r,T3,R1}$	-1.49469×10^{-6}	2.12448×10^{-6}
$P^{(2)}_{r,T3,R3}$	3.30340×10^{-7}	-4.52386×10^{-7}
$P^{(2)}_{r,T3,R5}$	2.09856×10^{-7}	-2.89522×10^{-7}
$P^{(2)}_{r,T5,R1}$	2.38981×10^{-7}	-3.41404×10^{-7}
$P^{(2)}_{r,T5,R3}$	2.10087×10^{-7}	-2.89170×10^{-7}
$P^{(2)}_{r,T5,R5}$	1.18741×10^{-7}	-1.64652×10^{-7}

Table 2 Subcomponents of $P_r^{(4)}$ (Unit: [W]).

	13.17 MHz	13.85 MHz
$P^{(4)}_{r,T0,T0}$	6.11897×10^{-7}	4.29813×10^{-6}
$P^{(4)}_{r,T0,T1}$	-1.21981×10^{-5}	-7.29486×10^{-5}
$P^{(4)}_{r,T0,T3}$	-3.83237×10^{-7}	-2.19966×10^{-6}
$P^{(4)}_{r,T0,T5}$	-7.10250×10^{-8}	-4.09563×10^{-7}
$P^{(4)}_{r,T1,T1}$	2.18545×10^{-4}	3.46815×10^{-4}
$P^{(4)}_{r,T1,T3}$	1.37658×10^{-5}	2.09247×10^{-5}
$P^{(4)}_{r,T1,T5}$	2.55334×10^{-6}	3.89614×10^{-6}
$P^{(4)}_{r,T3,T3}$	2.16614×10^{-7}	3.15385×10^{-7}
$P^{(4)}_{r,T3,T5}$	8.02309×10^{-8}	1.17265×10^{-7}
$P^{(4)}_{r,T5,T5}$	7.40424×10^{-9}	1.08636×10^{-8}
$P^{(4)}_{r,R0,R0}$	1.35174×10^{-6}	1.53755×10^{-6}
$P^{(4)}_{r,R0,R1}$	-1.52609×10^{-5}	-2.04935×10^{-5}
$P^{(4)}_{r,R0,R3}$	-4.79058×10^{-7}	-6.17794×10^{-7}
$P^{(4)}_{r,R0,R5}$	-8.86969×10^{-8}	-1.14972×10^{-7}
$P^{(4)}_{r,R1,R1}$	1.10122×10^{-4}	1.64432×10^{-4}
$P^{(4)}_{r,R1,R3}$	6.92896×10^{-6}	9.93339×10^{-6}
$P^{(4)}_{r,R1,R5}$	1.28448×10^{-6}	1.85087×10^{-6}
$P^{(4)}_{r,R3,R3}$	1.08915×10^{-7}	1.49910×10^{-7}
$P^{(4)}_{r,R3,R5}$	4.03178×10^{-8}	5.57775×10^{-8}
$P^{(4)}_{r,R5,R5}$	3.71870×10^{-9}	5.17096×10^{-9}
$P^{(4)}_{r,T0,R0}$	8.19578×10^{-7}	1.90358×10^{-6}
$P^{(4)}_{r,T0,R1}$	-1.60646×10^{-5}	2.50875×10^{-5}
$P^{(4)}_{r,T0,R3}$	-5.05645×10^{-7}	7.60304×10^{-7}
$P^{(4)}_{r,T0,R5}$	-9.37766×10^{-8}	1.42006×10^{-7}
$P^{(4)}_{r,T1,R0}$	-3.42455×10^{-5}	-2.07284×10^{-6}
$P^{(4)}_{r,T1,R1}$	2.14677×10^{-4}	-3.51228×10^{-4}
$P^{(4)}_{r,T1,R3}$	6.74013×10^{-6}	-1.06247×10^{-5}
$P^{(4)}_{r,T1,R5}$	1.24767×10^{-6}	-1.98134×10^{-6}
$P^{(4)}_{r,T3,R0}$	-1.07879×10^{-6}	-6.03870×10^{-8}
$P^{(4)}_{r,T3,R1}$	6.74932×10^{-6}	-1.06094×10^{-5}
$P^{(4)}_{r,T3,R3}$	2.11543×10^{-7}	-3.20388×10^{-7}
$P^{(4)}_{r,T3,R5}$	3.90164×10^{-8}	-5.95301×10^{-8}
$P^{(4)}_{r,T5,R0}$	-2.00147×10^{-7}	-1.10867×10^{-8}
$P^{(4)}_{r,T5,R1}$	1.25074×10^{-6}	-1.97607×10^{-6}
$P^{(4)}_{r,T5,R3}$	3.90595×10^{-8}	-5.94577×10^{-8}
$P^{(4)}_{r,T5,R5}$	7.14774×10^{-9}	-1.09613×10^{-8}

6. Conclusion

In this paper, the basic source of undesired radiation in WPT systems was elucidated by use of IEM. The currents on the coils were expanded into the Fourier basis functions, and several analytical expressions for the self- and mutual impedance components between the basis functions were derived. It was noted that the self-impedance components that are proportional to s^2 correspond to the radiation resistance of the equivalent infinitesimal dipoles of the basis functions, as described in the previous reports. In addition, it was shown that the self-impedance components that are proportional to s^4 correspond to the radiation resistance of the equivalent infinitesimal loops of the basis functions.

Subsequently, the S-parameters between the Tx and Rx ports, the radiated power, and the conduction loss power were numerically calculated. The results by the IEM and the full-wave MoM agree with each other, which confirms the validity of both the methods.

Further, the radiated power components $P_r^{(2)}$ and $P_r^{(4)}$, which are due to the impedance components proportional to s^2 and s^4, respectively, are maximum at different frequencies. At the frequency at which the component $P_r^{(2)}$ is maximum, the radiations due to the equivalent infinitesimal dipoles of the currents on the coils are enhanced. On the other hand, at the frequency at which the component $P_r^{(4)}$ is maximum, the radiations due to the equivalent infinitesimal loops of the currents on the coils are enhanced. Furthermore, because the total radiated power $P_r = P_r^{(2)} + P_r^{(4)}$ obtained by the IEM agrees with that yielded by the full-wave MoM, it can be concluded that the undesired radiations in the WPT system consist of those due to the equivalent dipoles and loops of the currents on the coils.

Incidentally, an equivalent circuit model of the WPT system can be obtained by using the self- and mutual impedance components derived by the IEM. Unfortunately, the scale of the equivalent circuit is not so small because the total number of basis functions is $2 + 2N_F = 52$. However, a small-scale equivalent circuit can be obtained by expanding the currents on conductors into a few dominant eigenmodes. The details will be discussed in further studies.

References

[1] A. Karalis, J.D. Joannopoulos, and M. Soljačić, "Efficient wireless non-radiative mid-range energy transfer," Annals of Physics, vol.323, pp.34–48, 2008. DOI: 10.1016/j.aop.2007.04.017
[2] N. Haga and M. Takahashi, "Circuit modeling technique for electrically-very-small devices based on Laurent series expansion of self-/mutual impedances," IEICE Trans. Commun., vol.E101-B, no.2, pp.555–563, Feb. 2018. DOI: 10.1587/transcom.2017EBP3196
[3] N. Haga and M. Takahashi, "Passive element approximation of equivalent circuits by the impedance expansion method," IEICE Trans. Commun., vol.E101-B, no.4, pp.1069–1075, April 2018. DOI: 10.1587/transcom.2017EBP3246
[4] R.F. Harrington, Field Computation by Moment Methods, Macmillan, New York, NY, USA, 1965.
[5] H. Hirayama, T. Ozawa, Y. Hiraiwa, N. Kikuma, and K. Sakakibara, "A consideration of electro-magnetic-resonant coupling mode in wireless power transmission," IEICE Electron. Express, vol.6, no.19, pp.1421–1425, Oct. 2009. DOI: 10.1587/elex.6.1421
[6] C.A. Balanis, Antenna Theory: Analysis and Design, 4th ed., John Wiley & Sons, Hoboken, NJ, USA, 2016.
[7] H. Takahasi and M. Mori, "Double exponential formulas for numerical integration," Publ. Res. Inst. Math. Sci., vol.9, no.3, pp.721–741, 1973.

Appendix: Basis Functions for Full-Wave MoM

The basis function $\boldsymbol{F}_m(\boldsymbol{r})$ for the full-wave MoM is defined over two neighboring quadrangular segments S_m^- and S_m^+, which are shown in Fig. A· 1. The segment S_m^- is formed by vertices $\boldsymbol{a}_m^-$, $\boldsymbol{b}_m^-$, $\boldsymbol{c}_m^-$, and $\boldsymbol{d}_m^-$. Similarly, the segment S_m^+ is formed by vertices $\boldsymbol{a}_m^+$, $\boldsymbol{b}_m^+$, $\boldsymbol{c}_m^+$, and $\boldsymbol{d}_m^+$. To define the basis function, the position $\boldsymbol{r}_m^\pm$ on $S_m^\pm$ is first expressed in terms of parametric variables u and v, as follows:

$$\boldsymbol{r}_m^\pm = (1-u)(1-v)\boldsymbol{a}_m^\pm + u(1-v)\boldsymbol{b}_m^\pm + uv\boldsymbol{c}_m^\pm + (1-u)v\boldsymbol{d}_m^\pm, \quad (\mathrm{A}\cdot 1)$$

where $0 \le u \le 1$ and $0 \le v \le 1$. The basis function $\boldsymbol{F}_m(\boldsymbol{r})$ is defined as follows:

$$\boldsymbol{F}_m(\boldsymbol{r}) = \begin{cases} u\dfrac{\partial \boldsymbol{r}_m^-}{\partial u}\left|\dfrac{\partial \boldsymbol{r}_m^-}{\partial u}\times\dfrac{\partial \boldsymbol{r}_m^-}{\partial v}\right|^{-1}, & \boldsymbol{r}\in S_m^- \\ -u\dfrac{\partial \boldsymbol{r}_m^+}{\partial u}\left|\dfrac{\partial \boldsymbol{r}_m^+}{\partial u}\times\dfrac{\partial \boldsymbol{r}_m^+}{\partial v}\right|^{-1}, & \boldsymbol{r}\in S_m^+ \end{cases}. \quad (\mathrm{A}\cdot 2)$$

If both S_m^- and S_m^+ are rectangles, $\boldsymbol{F}_m(\boldsymbol{r})$ is equivalent to the so-called rooftop function.

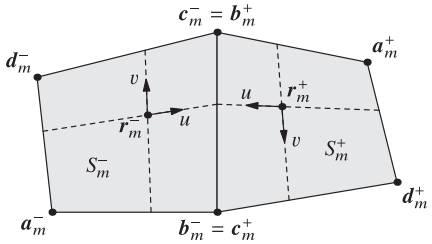

Fig. A· 1 Two neighboring quadrangular segments S_m^- and S_m^+.

Nozomi Haga was born in Yamagata, Japan, in January 1985. He received the B.E., M.E., and D.E. degrees from Chiba University, Chiba, Japan, in 2007, 2009, and 2012, respectively. He is currently an Assistant Professor at Gunma University, Gunma, Japan. His main interests have been electrically small antennas and evaluation of body-centric wireless communication channels. He received the IEICE Technical Committee on Antennas and Propagation Young Researcher Award in 2012. He is a member of the Institute of Electrical and Electronics Engineers (IEEE).

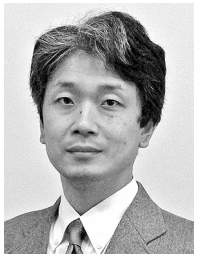

Masaharu Takahashi was born in Chiba, Japan, in December 1965. He received the B.E. degree in electrical engineering from Tohoku University, Miyagi, Japan, in 1989, and the M.E. and D.E. degrees in electrical engineering from the Tokyo Institute of Technology, Tokyo, Japan, in 1991 and 1994, respectively. From 1994 to 1996, he was a Research Associate, and from 1996 to 2000, an Assistant Professor with the Musashi Institute of Technology, Tokyo, Japan. From 2000 to 2004, he was an Associate Professor with the Tokyo University of Agriculture and Technology, Tokyo, Japan. He is currently an Associate Professor with the Research Center for Frontier Medical Engineering, Chiba University, Chiba, Japan. His main interests are electrically small antennas, planar array antennas, and EM compatibility. He was the recipient of the 1994 IEEE Antennas and Propagation Society (IEEE AP-S) Tokyo Chapter Young Engineer Award.